

Highly luminescent and stable layered perovskite as the emitter for light emitting diodes

Mingyang Wei¹, Weihai Sun¹, Yang Liu², Zhiwei Liu², Lixin Xiao^{1,3}, Zuqiang Bian², and Zhijian Chen^{*,1,3}

¹ State Key Laboratory for Mesoscopic Physics and Department of Physics, Peking University, Beijing 100871, P.R. China

² Beijing National Laboratory for Molecular Sciences, State Key Laboratory of Rare Earth Materials Chemistry and Applications, College of Chemistry and Molecular Engineering, Peking University, Beijing 100871, P.R. China

³ Co-Innovation Center for Micro/Nano Optoelectronic Materials and Devices, Chongqing University of Arts and Sciences, Yongchuan Chongqing 402160, P.R. China

Received 30 March 2016, revised 5 May 2016, accepted 25 May 2016

Published online 9 June 2016

Keywords layered perovskite, PeLEDs, quantum wells exciton recombination

* Corresponding author: e-mail zjchen@pku.edu.cn, Phone: +86-10-6275-4990, Fax: +86-10-6275-6567

Air instability and poor exciton recombination of 3D perovskites MAPbX_3 ($\text{MA} = \text{CH}_3\text{NH}_3$, $\text{X} = \text{halogens}$) seriously hinder their applications in light emitting diodes. Herein, we report a promising alternative to solve these two critical drawbacks. Layered perovskite $\text{OA}_2(\text{MA})_{n-1}\text{Pb}_n\text{Br}_{3n+1}$ ($\text{OA} = \text{C}_8\text{H}_{17}\text{NH}_3$) has higher binding energy and is passivated by long organic chain, which can be synthesized using a facile method. By increasing the OA^+ ratio in layered perovskite, strong quantum confinement effect and obvious features of exciton were observed in photoluminescence and UV-Vis absorption spectra. Notably, the photoluminescence quantum yield (PLQY) of $(\text{OA})_2(\text{MA})_2\text{Pb}_3\text{Br}_{10}$ ($n=3$ layered

perovskite) can be up to 67.3% due to the enhanced exciton recombination, significantly higher than its 3D counterpart. Moreover, layered perovskite exhibits promoted stability in air than that of the 3D perovskite. The layered perovskite $(\text{OA})_2(\text{MA})_2\text{Pb}_3\text{Br}_{10}$ -based perovskite light emitting diodes (PeLEDs) with a maximum current efficiency, a maximum power efficiency and the external quantum efficiency (EQE) of 1.43 cd A^{-1} , 0.89 lm W^{-1} , and 0.53% was demonstrated, which can be compared with that of the best-reported perovskite quantum dots LEDs so far. The demonstration of layered perovskite renders its bright future in optoelectronic applications, such as displays and photodetections.

© 2016 WILEY-VCH Verlag GmbH & Co. KGaA, Weinheim

1 Introduction Organic–inorganic hybrid perovskites MAPbX_3 ($\text{MA} = \text{CH}_3\text{NH}_3$, $\text{X} = \text{halogens}$) have been employed as an important absorber for solar cells [1–3] due to its low cost and excellent optoelectronic properties such as long charge carrier diffusion length and high charge carrier mobility (for solution-processed semiconductors) [4, 5], which have made the power conversion efficiency (PCE) of perovskite solar cell surpass 20% [6]. In addition, the excellent photoluminescence (PL) properties of the organic–inorganic perovskites also make them as the potential emitter for light emitting diodes [7]. Thus, it has been seen the growing interests for perovskite light emitting diodes (PeLEDs) since 2014 [7–11].

Unfortunately, two intrinsic problems of perovskite have largely limited the potential of PeLEDs, which are weak exciton recombination [12–14] and poor stability

[15, 16] of perovskite MAPbX_3 . In order to obtain highly efficient PeLEDs, many works have been done to solve the first problem such as the synthesis of perovskite quantum dots (QDs) [17, 18] and the nanograin engineering of perovskite thin films [19]. With unremitting efforts, the photoluminescence quantum yield (PLQY) of perovskite QDs have already approached unity [18, 20], and the current efficiency of PeLEDs with 42.9 cd A^{-1} could be achieved by the nanograin engineering [19], which is comparable with the phosphorescent OLEDs. However, the stability issue has not been apparently improved due to the instable nature of perovskite QDs and thin films [21]. Thus, methods to enhance the exciton recombination and improve the stability of perovskite at the same time are strongly desired.

The layered perovskite may be a good candidate for chemically stable and high-efficiency PeLEDs. Layered

perovskite is the 2D counterpart of bulk perovskite MAPbX_3 . It is achieved by partially substituting the short organic cation MA^+ ($\text{MA}^+ = \text{CH}_3\text{NH}_3^+$) with the long organic cation such as OA^+ ($\text{OA}^+ = \text{C}_8\text{H}_{17}\text{NH}_3^+$) so that the inorganic layers are separated into two-dimensional form [22]. When increasing the ratio of OA^+ in layered perovskite, each inorganic layer will contain less corner-shared inorganic octahedral layers as shown in Fig. 1a, leading to the thinner inorganic layer and stronger quantum confinement effect [23, 24]. Therefore, layered perovskite can have strong exciton recombination under high OA^+ concentration [24]. Furthermore, the stability of layered perovskite is better than 3D perovskite MAPbX_3 due to the large van der Waals force of OA^+ [25]. As a result, layered perovskite could be an ideal alternative to enhance the exciton recombination and stability of perovskite simultaneously.

In this work, we systematically studied the influence of OA^+ ratio of layered perovskite on the optical properties and explored its potential for optoelectronic devices. By properly controlling OA^+ ratio, the PLQY of layered perovskite can be up to 70 %. More encouragingly, the photoluminescence (PL) intensity of layered perovskite remained almost unchanged without special protective measures after a week in chlorobenzene, while the quenching of 3D perovskite was obvious with time. Finally, we fabricated light emitting diodes using layered perovskite as emitter whose device performance has already been comparable with perovskite QDs-based PeLEDs. These results suggest the promising future of layered perovskite for optoelectronic applications.

2 Experimental

2.1 Synthesis of MABr and OABr MABr was synthesized by reacting methylamine (33 wt.% in ethanol) and hydrobromic acid (48 wt.% in water) with the molar ratio of 1:1 in an ice bath for 2 h with stirring followed by vacuum drying and washing with diethyl. OABr were prepared using the same method by mixing n-octylamine and hydrobromic acid in a 1:1 molar ratio.

2.2 Synthesis of layered perovskite MABr, OABr, PbBr_2 (22.02 mg) was dissolved in 1 ml dimethylformamide

(DMF) to form clear precursors with molar ratio of three solutes following the structure formula of layered perovskite $(\text{OA})_2(\text{MA})_{n-1}\text{Pb}_n\text{Br}_{3n+1}$ ($n = 2, 3, 4, 5, \infty$). Then 0.1 ml precursor was dipped into 10 ml chlorobenzene under vigorous stirring to induce the formation of layered perovskite. Notably, no oleic acid was injected into chlorobenzene during the synthesis of layered perovskite. For $(\text{OA})_2\text{PbBr}_4$, the concentration was ten times smaller in order to form stable dispersion. $(\text{OA})_2\text{MAPb}_2\text{Br}_{7-x}\text{Cl}_x$ was synthesized using the same method while the solutes were changed to MABr, OABr, PbBr_2 , and PbCl_2 with the molar ratio depending on the structure formula of the wanted dispersion. The concentration of $(\text{OA})_2\text{MAPb}_2\text{Br}_7$ in chlorobenzene was controlled by changing the concentration of precursors in DMF with the following procedure remain the same.

2.3 Characterization of layered perovskite UV-Vis spectra were measured using a Shimadzu UV-3150 UV-Vis/NIR spectrophotometer. PL spectra ($\lambda_{\text{exc}} = 350 \text{ nm}$) were obtained using a FluroMax-2 (Jobin-Yvon-Spex) luminescence spectrometer. PLQY was measured on a Nanolog FL3-2iHR spectrometer with an integrating sphere. Structure analysis of layered perovskite samples were carried out by X-ray diffractometer (XRD, Philips Xpert) using Ni filtered CuK_α ($\lambda = 0.154 \text{ nm}$, radiation at 45 KV and 40 mA). The samples were prepared on quartz by spin-coating the layered perovskite dispersion (0.02 M in toluene) at a rate of 3000 rpm for 60 s, and cured at 110°C for 10 min.

2.4 Device fabrication and characterization The ITO substrates were cleaned by sonication sequentially in deionized water, acetone, and isopropyl alcohol. The PEDOT:PSS (Clevios P VP Al 4083) layer was spin-coated on the UV-ozone-treated ITO substrates at a spin rate of 3000 rpm for 30 s and dried at 140°C for 10 min in air. Then the substrates were transformed into a N_2 -filled glovebox. The Poly-TPD dissolved in chlorobenzene (10 mg ml^{-1}) was also spin-coated on the PEDOT:PSS layer at 2000 rpm for 60 s, followed by thermal annealing at 110°C for 30 min. The layered perovskite layer was then deposited on the ITO/PEDOT:PSS/poly-TPD layer by spin-coating the layered

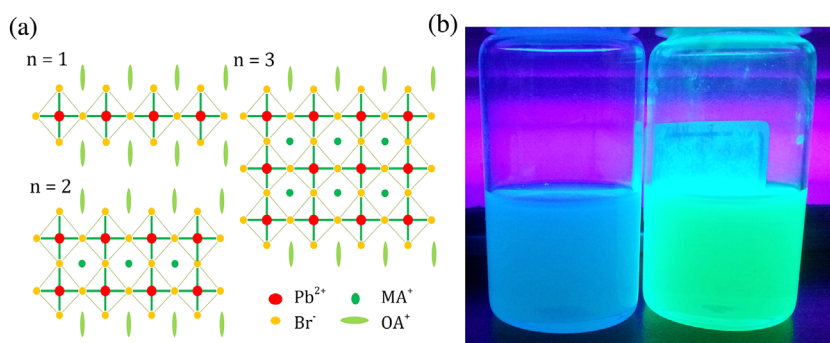


Figure 1 (a) Structure of layered perovskites $(\text{OA})_2(\text{MA})_{n-1}\text{Pb}_n\text{Br}_{3n+1}$ ($n = 1, 2, 3$). (b) The samples of layered perovskite $(\text{OA})_2\text{MAPb}_2\text{Br}_7$ (left) and $(\text{OA})_2(\text{MA})_2\text{Pb}_3\text{Br}_{10}$ (right) in chlorobenzene under UV excitation.

perovskite dispersion (0.02 M in toluene) at a rate of 3000 rpm for 60 s, and cured at 110 °C for 10 min. The 40 nm TmPyPB, 1 nm LiF, and 100 nm Al layers were thermally deposited under a base pressure of 3×10^{-6} Torr at deposition rates (monitored with a quartz-oscillator) of 1 Å s^{-1} for TmPyPB, 0.1 Å s^{-1} for LiF, and $4\text{--}5 \text{ Å s}^{-1}$ for the Al layer with a device active area of 1 mm^2 . The EL spectra were measured with a PR-650 spectrofluorometer by continually increasing the applied bias voltage using a Keithley 2611 System SourceMeter.

3 Results and discussion Layered perovskite was synthesized under a facile method. OABr, MABr, PbBr₂ (0.06 M) were dissolved in good solvent N, N-dimethylformamide (DMF) to form clear precursors. The molar ratio of three solutes is determined by the wanted structure formula of layered perovskite $(\text{OA})_2(\text{MA})_{n-1}\text{Pb}_n\text{Br}_{3n+1}$ where n represents the number of lead bromide octahedral layers contained in an individual inorganic layer. For 3D perovskite, $n = \infty$ while for the thinnest 2D inorganic layer, $n = 1$. Then 0.1 ml precursors were dropped into 10 ml poor solvent chlorobenzene to form layered perovskite dispersions as shown in Fig. 1b. For $n = 2, 3, 4, 5, \infty$, layered perovskite dispersions can exist very stably in chlorobenzene. But for $n = 1$, the solution tended to be cloudy in several minutes under the same concentration. Only the concentration of $(\text{OA})_2\text{PbBr}_4$ was ten times smaller, it can exist stably in chlorobenzene. Notably the synthesis procedure for layered perovskite $(\text{OA})_2(\text{MA})_{n-1}\text{Pb}_n\text{Br}_{3n+1}$ is simpler than the fabrication of all-inorganic perovskite CsPbBr₃ QDs where the typical reaction temperature is as high as 170 °C [18]. The structure of the layered perovskite synthesized was analyzed by XRD as shown in Fig. S1 (see Supporting Information (SI), online at: www.pss-a.com), which corresponds well with the

previous results [23, 24] mentioned in Section 1 and structure illustrations shown in Fig. 1a. A more detailed discussion can be found in the Supporting Information.

Using the layered perovskite $(\text{OA})_2(\text{MA})_{n-1}\text{Pb}_n\text{Br}_{3n+1}$ ($n = 1, 2, 3, 4, 5, \infty$) dispersions, we studied the effects of the thickness of each inorganic layer on the optical properties by measuring the UV-Vis absorption spectra and PL spectra. In Fig. 2a, when n was decreased from ∞ to 1 which means each inorganic layer became thinner, the PL peak of layered perovskite was shifted from 544 to 441 nm. This blue shift of spectra can be explained by the quantum confinement effect. Since charge carriers mainly move in the inorganic layer of layered perovskite while the OA^+ cations are the insulating layer [24], each inorganic layer in layered perovskite can be regarded as the quantum well and the thickness of each quantum well is tuned by the number of lead bromide octahedral layers each inorganic layer contains. Thus, thinner inorganic layer will lead to the enhancement of quantum confinement effect which is common for the quantum well [26], resulting in the blue shift of spectra. It is obvious that quantum confinement effect is the intrinsic property of layered perovskite which can even exist in bulk materials. However, for perovskite QDs, the quantum confinement effect is arisen from the size effect of each particle [18]. Compared with the difficulty of controlling the particle size of perovskite QDs, the synthesis of layered perovskite has higher reproducibility.

Furthermore, it can be found that the full width at half maximum (FWHM) of PL for layered perovskite ($n = 1, 3, 4$) is very narrow ($\sim 25 \text{ nm}$), which is appropriate for high color purity phosphors [21]. But for $n = 2$ layered perovskite, two emission peaks appeared in PL spectra (Fig. 2a). Interestingly, the proportion of the intensity for two peaks was influenced by the concentration of layered perovskite solution (Fig. S2, SI). It has been reported [27]

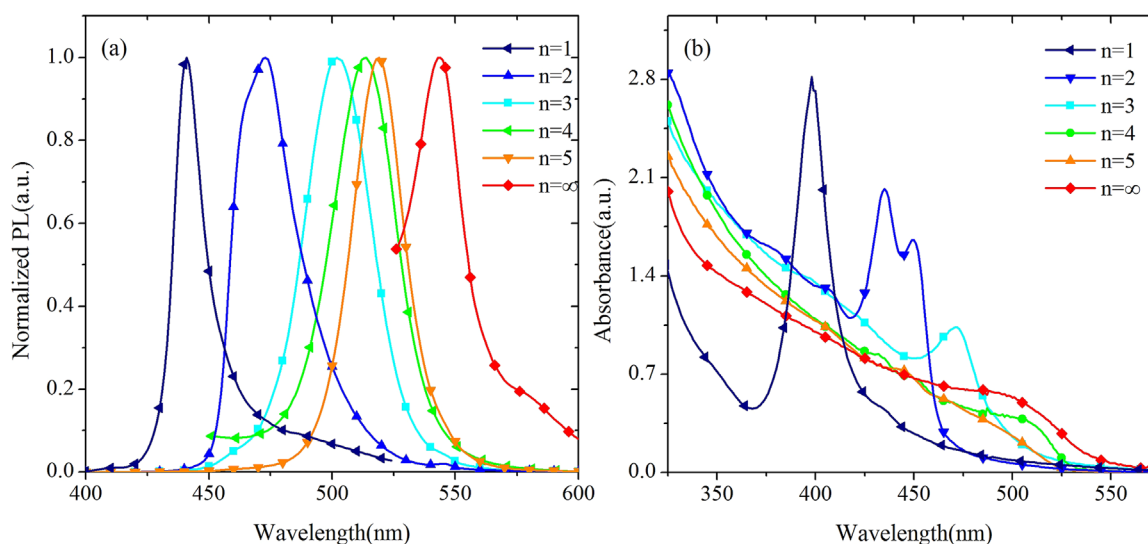


Figure 2 (a) PL spectra and (b) UV-Vis absorption spectra of layered perovskite $(\text{OA})_2(\text{MA})_{n-1}\text{Pb}_n\text{Br}_{3n+1}$ ($n = 1, 2, 3, 4, 5, \infty$).

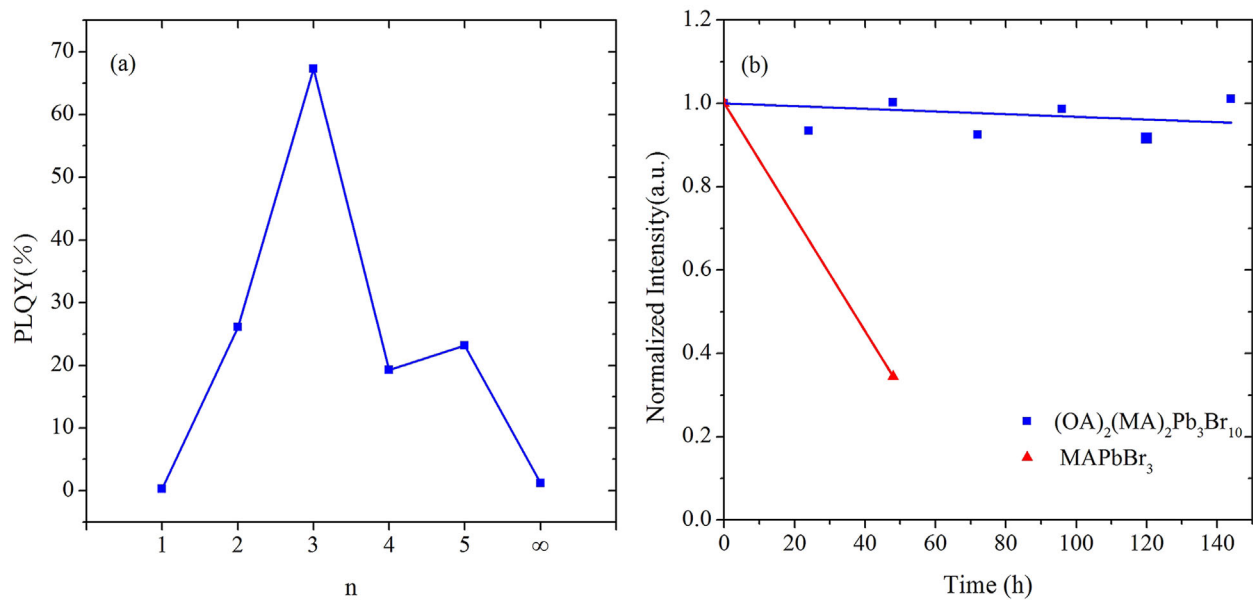


Figure 3 (a) PLQY of layered perovskite $(\text{OA})_2(\text{MA})_{n-1}\text{Pb}_3\text{Br}_{3n+1}$, (b) PL intensity of layered perovskite for $n=3$ tested every 24 h, comparing with its 3D counterpart.

that the structure distortion can occur when the number of stacked inorganic layers is varied. Considering the number of stacked layers relates closely with the solution concentration, we speculated two structure phases of layered perovskite co-exist in dispersions which caused the broadening of PL spectra. However, it needs further explanation why such phenomenon happened uniquely for $n=2$ layered perovskite. The more explicit study is currently underway.

In layered perovskite, electrons and holes are more tightly bonded than 3D perovskite since they are all confined in a thin inorganic layer owing to the intrinsic quantum well structure [26, 28]. Thus, we can expect layered perovskite has higher exciton binding energy and more significant exciton recombination than 3D perovskite, which are crucial for the development of PeLEDs [19]. Indeed as shown in Fig. 2b, there is no sign of exciton absorption peak near the band edge of absorption spectra when $n=4, 5, \infty$ due to the loose bond, but when we further reduced the thickness of each quantum well ($n=1, 2, 3$), exciton absorption peak can be clearly observed, suggesting the existence of significant exciton recombination. Again we can find two exciton absorption peaks for $n=2$ in accordance with the two emission species in PL spectra. By proper fitting of the absorption data (Fig. S3, SI), we calculated that the exciton binding energy for $n=1$ is as high as 510 meV, which is nearly sixfold enlargement for that of 3D perovskite (84 meV) and much higher than the kinetic energy under ambient temperature (26 meV) [29]. Even though this high binding energy is favorable for PeLEDs, the cloudy phenomenon for the $n=1$ layered perovskite under high concentration in chlorobenzene may indicate $n=2$ or $n=3$

layered perovskite is more suitable than all OA^+ -substituted layered perovskite for optoelectronic applications considering their exciton features are already clear.

The PLQY measurements were also conducted to find out whether there is an optimum value of n for optoelectronic applications, as shown in Fig. 3a. For 3D perovskite, its PLQY is less than 1% suggesting poor crystal quality and dominant nonradiative recombination. After the incorporation of OA^+ , the PLQY of layered perovskite increases significantly. For $n=4$ and 5, PLQYs reach 20%, which may be caused purely by the protective effect of long

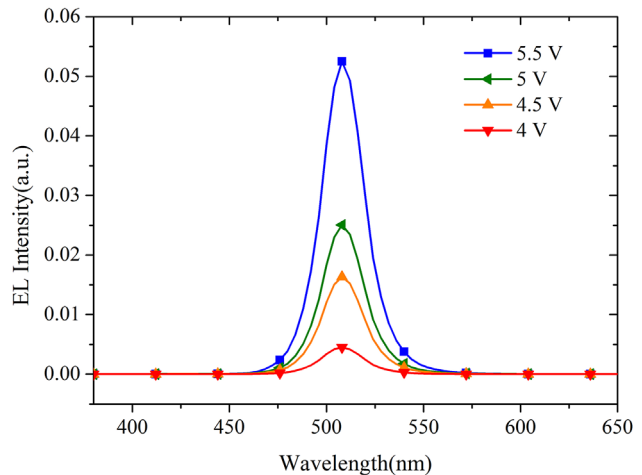


Figure 4 EL spectra of layered perovskite LEDs under different applied bias voltages.

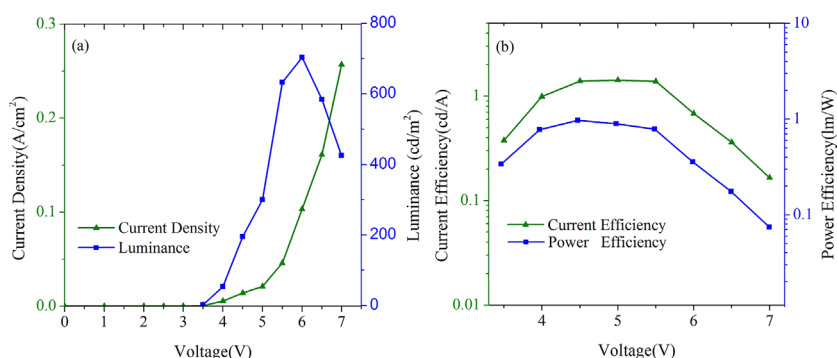


Figure 5 (a) J - V characteristics, luminance- V characteristics, (b) current efficiency and power efficiency as a function of voltage for layered perovskite LEDs.

organic chains [18] since the exciton features are not very clear for $n = 4$ and 5. But for $n = 3$ layered perovskite where exciton features start to be exhibited, the strong exciton recombination and the protective effect of long organic chain may both help the PLQY reach up to 67.3% which is already comparable with MAPbBr₃ QDs and nonshelled CdSe QDs [17]. It needs to note that there is still room to improve the PLQY of layered perovskite by purification and surface passivation. However, when n is below 3, the PLQY of perovskite gradually decreased even though the exciton binding energy is higher than that of layered perovskite for $n \geq 3$. Therefore, we suggested under high OA⁺ ratio, layered perovskite may not maintain very high crystal quality leading to the rapid quenching.

For PeLEDs, the stability of perovskite is another most important issue we primarily concern as mentioned in the introduction part. Since the strong van der Waals force in the existence of long organic chain can effectively stabilize perovskite materials [25], we expected (OA)₂(MA)₂Pb₃Br₁₀ had prolonged longevity compared with 3D perovskite. Encouragingly, the PL intensity of layered perovskite (OA)₂(MA)₂Pb₃Br₁₀ exhibited no apparent decrease within 1 week (Fig. 3b). Meanwhile, the PL intensity of 3D perovskite was only 30% of the original value after 50 h, indicating the layered perovskite has much better stability than that of 3D perovskite. The enhanced stability as well as the stronger exciton recombination of (OA)₂(MA)₂Pb₃Br₁₀ compared with 3D perovskite suggests it can be an ideal emitter for PeLEDs in consideration of device lifetime and efficiency.

Finally, we fabricated device by using (OA)₂(MA)₂Pb₃Br₁₀ as the emitter for PeLEDs. The device structure is

designed in the following structure: ITO/PEDOT:PSS/Poly-TPD/(OA)₂(MA)₂Pb₃Br₁₀/TmPyPB/LiF/Al. The PEDOT:PSS layer and Poly-TPD layer serve as the hole transporting layers (HTLs) when TmPyPB layer serves as the electron transporting layer (ETL). Layered perovskite layer (0.02 M in toluene) was spin-coated onto the Poly-TPD. This simple structure is typically used for solution-processed LEDs [30]. The detailed fabrication methods are shown in Section 2. As shown in Fig. 4, we observed green electroluminescence which centered at 508 nm under applied bias voltage higher than 3.5 V. No wavelength shift of EL spectra could be observed under different applied bias voltage and the FWHM of EL spectra is also very narrow (27 nm). The maximum luminance of 704 cd/m² was obtained at 6 V as shown in Fig. 5a. After 6 V, the luminance of device gradually faded. The current efficiency and power efficiency of the device is exhibited in Fig. 5b. The device reached its maximum current efficiency of 1.43 cd/A and the maximum power efficiency of 0.89 lm/W at 4.5 V with the external quantum efficiency (EQE) of 0.53%.

In Table 1, we compared our device performance with that of perovskite QDs-based PeLEDs in the literatures [31–34]. It can be seen that our device performance has already been comparable with that of CsPbBr₃ QDs-based PeLEDs and MAPbBr₃ QDs-based PeLEDs reported so far. But considering the high PLQY of perovskite QDs [17, 18, 32] and layered perovskite reported in this work, none of these devices reached their full potential. The further research for raising the device performance will focus on the optimization of surface coverage and balancing the injection of charge carriers. Furthermore, the layered perovskite (OA)₂(MA)₂Pb₃Br₁₀ could be an alternative

Table 1 Comparison of device performances of layered perovskite LEDs and perovskite QDs LEDs.

emitter	λ_{max} (FWHM) (nm)	V_{on} (V)	max. EQE (%)	max. CE (cd/A)	max. L (cd/m ²)	Ref.
MAPbBr ₃ QDs	524 (24)	2.9	1.1	4.5	250	[31]
CsPbBr ₃ QDs	514 (23)	4.2	0.12	0.43	946	[32]
CsPbBr ₃ QDs	527 (18)	3.0	0.008	0.035	407	[33]
CsPbBr ₃ QDs	516 (18)	2.5	0.06	0.19	1377	[34]
(OA) ₂ (MA) ₂ Pb ₃ Br ₁₀	508 (27)	3.5	0.53	1.43	704	this work

candidate for other optoelectronic applications such as photodetectors or phototransistors in consideration of its long-term stability and strong exciton recombination. The relevant works are also being conducted.

4 Conclusions In summary, we synthesized layered perovskite $(\text{OA})_2(\text{MA})_{n-1}\text{Pb}_n\text{Br}_{3n+1}$ ($n = 1, 2, 3, 4, 5, \infty$) by partially replacing MA^+ with OA^+ in perovskite precursor. By increasing the ratio of OA^+ in perovskite, the blue shift was observed in PL spectra as well as in absorption spectra, which is ascribed to the enhancement of quantum confinement effect. It is noteworthy that the PLQY of layered perovskite $(\text{OA})_2(\text{MA})_2\text{Pb}_3\text{Br}_{10}$ is as high as 67.3%, which is near to the value of MAPbBr_3 QDs. Furthermore, we have demonstrated organic–inorganic hybrid PeLEDs with a sharp green emission (FWHM = 27 nm) by employing the layered perovskite $(\text{OA})_2(\text{MA})_2\text{Pb}_3\text{Br}_{10}$ as an emitter and obtained the maximum current efficiency of 1.43 cd/A, which has an almost equal value with the PeLEDs based on perovskite QDs. Especially to deserve to be mentioned, the layered perovskite showed a higher stability than that of 3D perovskite, indicating it could be a potential substitution in optoelectronic applications such as LEDs, phosphors, and photodetectors.

Supporting Information Additional supporting information may be found in the online version of this article at the publisher's web-site.

Acknowledgements We acknowledge the financial support from the National Natural Science Foundation of China (11574009). M. Wei is also supported by the President's Fund for Undergraduate Research of Peking University.

References

- [1] H. Kim, C. Lee, J. Im, K. Lee, T. Moehl, A. Marchioro, S. J. Moon, R. Humphry-Baker, J. Yum, J. E. Moser, M. Grätzel, and N. Park, *Sci. Rep.* **2**, 591 (2012).
- [2] J. Burschka, N. Pellet, S. J. Moon, R. Humphry-Baker, P. Gao, M. K. Nazeeruddin, and M. Grätzel, *Nature* **499**, 316 (2013).
- [3] M. Lee, J. Teuscher, T. Miyasaka, T. N. Murakami, and H. J. Snaith, *Science* **338**, 643 (2012).
- [4] S. D. Stranks, G. E. Eperon, G. Grancini, C. Menelaou, M. J. Alcocer, T. Leijtens, L. M. Herz, A. Petrozza, and H. J. Snaith, *Science* **342**, 341 (2013).
- [5] D. Shi, V. Adinolfi, R. Comin, M. Yuan, E. Alarousu, A. Buin, Y. Chen, S. Hoogland, A. Rothenberger, K. Katsiev, Y. Losovyj, X. Zhang, P. A. Dowben, O. F. Mohammed, E. H. Sargent, and O. M. Bakr, *Science* **347**, 519 (2015).
- [6] W. Yang, J. Noh, N. Jeon, Y. Kim, S. Ryu, J. Seo, and S. Seok, *Science* **348**, 1234 (2015).
- [7] Z. Tan, R. S. Moghaddam, M. Lai, P. Docampo, R. Higler, F. Deschler, M. Price, A. Sadhanala, L. M. Pazos, D. Credgington, F. Hanusch, T. Bein, H. J. Snaith, and R. H. Friend, *Nature Nanotechnol.* **9**, 687 (2014).
- [8] J. Wang, N. Wang, Y. Jin, J. Si, Z. Tan, H. Du, L. Cheng, X. Dai, S. Bai, H. He, Z. Ye, M. Lai, R. H. Friend, and W. Huang, *Adv. Mater.* **27**, 2311 (2015).
- [9] Y. Kim, H. Cho, J. Heo, T. Kim, N. Myoung, C. Lee, S. Im, and T. Lee, *Adv. Mater.* **27**, 1248 (2015).
- [10] G. Li, Z. Tan, D. Di, M. Lai, L. Jiang, J. Lim, R. H. Friend, and N. C. Greenham, *Nano Lett.* **15**, 2640 (2015).
- [11] A. Wong, M. Lai, S. W. Eaton, Y. Yu, E. Lin, L. Dou, A. Fu, and P. Yang, *Nano Lett.* **15**, 5519 (2015).
- [12] J. S. Manser and P. V. Kamat, *Nat. Photon.* **8**, 737 (2014).
- [13] M. T. Trinh, X. Wu, D. Niesner, and X. Zhu, *J. Mater. Chem. A* **3**, 9285 (2015).
- [14] Y. Yang, M. Yang, Z. Li, R. Crisp, K. Zhu, and M. C. Beard, *J. Phys. Chem. Lett.* **6**, 4688 (2015).
- [15] O. Jaramillo-Quintero, R. Sanchez, M. Rincon, and I. Mora-Sero, *J. Phys. Chem. Lett.* **6**, 1883 (2015).
- [16] G. Niu, X. Guo, and L. Wang, *J. Mater. Chem. A* **3**, 8970 (2015).
- [17] F. Zhang, H. Zhong, C. Chen, X. Wu, X. Hu, H. Huang, J. Han, B. Zou, and Y. Dong, *ACS Nano* **9**, 4533 (2015).
- [18] L. Protesescu, S. Yakunin, M. I. Bodnarchuk, F. Krieg, R. Caputo, C. H. Hendon, R. Yang, A. Walsh, and M. V. Kovalenko, *Nano Lett.* **15**, 3692 (2015).
- [19] H. Cho, S. Jeong, M. Park, Y. Kim, C. Wolf, C. Lee, J. Heo, A. Sadhanala, N. Myoung, S. Yoo, S. Im, R. H. Friend, and T. Lee, *Science* **350**, 1222 (2015).
- [20] H. Huang, A. S. Susha, S. V. Kershaw, T. Hung, and A. L. Rogach, *Adv. Sci.* **2** (2015).
- [21] C. Lin, A. Meijerink, and R. Liu, *J. Phys. Chem. Lett.* **7**, 495 (2016).
- [22] D. B. Mitzi, C. A. Feild, W. T. A. Harrison, and A. M. Guloy, *Nature* **369**, 467 (1994).
- [23] X. Wu, M. T. Trinh, and X. Zhu, *J. Mater. Chem. C* **119**, 14714 (2015).
- [24] K. Abdel-Baki, F. Boitier, H. Diab, G. Lanty, K. Jemli, F. Lédée, D. Garrot, E. Deleporte, and J. Lauret, *J. Appl. Phys.* **119**, 064301 (2016).
- [25] D. Cao, C. C. Stoumpos, O. K. Farha, J. T. Hupp, and M. G. Kanatzidis, *J. Am. Chem. Soc.* **137**, 7843 (2015).
- [26] A. M. Fox, *Optical Properties of Solids*, Vol. 3 (Oxford University Press, USA, 2001).
- [27] W. Niu, A. Eiden, G. V. Prakash, and J. J. Baumberg, *Appl. Phys. Lett.* **104**, 171111 (2014).
- [28] J. A. Sichert, Y. Tong, N. Mutz, M. Vollmer, S. Fischer, K. Z. Milowska, R. García Cortadella, B. Nickel, C. Cardenas-Daw, J. K. Stolarczyk, A. S. Urban, and J. Feldmann, *Nano Lett.* **15**, 6521 (2015).
- [29] K. Zheng, Q. Zhu, M. Abdellah, M. E. Messing, W. Zhang, A. Generalov, Y. Niu, L. Ribaud, S. E. Canton, and T. Pullerits, *J. Phys. Chem. Lett.* **6**, 2969 (2015).
- [30] L. Qian, Y. Zheng, J. Xue, and P. H. Holloway, *Nature Photon.* **5**, 543 (2011).
- [31] H. Huang, F. Zhao, L. Liu, F. Zhang, X.-G. Wu, L. Shi, B. Zou, Q. Pei, and H. Zhong, *ACS Appl. Mater. Interf.* **7**, 28128 (2015).
- [32] J. Song, J. Li, X. Li, L. Xu, Y. Dong, and H. Zeng, *Adv. Mater.* **27**, 7162 (2015).
- [33] N. Yantara, S. Bhaumik, F. Yan, D. Sabba, H. A. Dewi, N. Mathews, P. P. Boix, H. V. Demir, and S. Mhaisalkar, *J. Phys. Chem. Lett.* **6**, 4360 (2015).
- [34] X. Zhang, H. Lin, H. Huang, C. Reckmeier, Y. Zhang, W. C. H. Choy, and A. L. Rogach, *Nano Lett.* **16**, 1415 (2016).